Proceedings of The 2016 IEEE International
Conference on Real-time Computing and Robotics
June 6-9, 2016, Angkor Wat, Cambodia

A Soft Robotic Glove for Hand Motion Assistance

Juan Yi, Zhong Shen, Chaoyang Song, Zheng Wang, *Member, IEEE*

***Abstract*—Soft robotic devices have the potential to be widely used in daily lives for their inherent compliance and adaptability, which result in high safety under unexpected situations. System complexity and requirements are much lower, comparing with conventional rigid-bodied robotic devices, which also result in significantly lower costs. This paper presents a robotic glove by utilizing soft artificial muscles providing redundant degrees of freedom (DOFs) to generate both flexion and extension hand motions for daily grasping and manipulation tasks. Different with the existing devices, to minimize the weight applied to the user's hands, pneumatic soft actuators were located on the fore arm and drive each finger via cable-transmission mechanisms. This actuation mechanism brings extra adaptability, motion smoothness, and user safety to the system. This design makes wearable robotic gloves more light-weight and user-friendly. Both theoretical and experimental analyses were conducted to explore the mechanical properties of pneumatic soft actuators. In addition, the fingertip trajectories were analyzed using Finite Element Methods, and a series of experiments were conducted evaluating both the technical and practical performances of the proposed glove.**

I. Introduction

Glove-type wearable robotic devices are developed to assist people with impaired hand functions both in their activities of daily living (ADLs) and in rehabilitation [1-12]. Most of such wearable robotic devices generate hand movements with linkage systems actuated by electrical motors which usually are heavy and inconvenient for using. Moreover, because of the human hand variation, most wearable robotic devices require customization in order to fulfill the geometrical fitting requirements between the exoskeleton device and the human hand joints. Approximating the high dexterity of human hands usually requires high complexity in both the mechanical and controller structures of the robotic systems, and hence also results in high costs for most users.

From a different approach, soft robotic devices become increasingly popular in recent years due to their high passive compliance for ensuring the users' safety, easy fabrication process, and low cost [5-12]. This also makes soft robots promising candidates for wearable assistive or rehabilitation devices [5, 6]. To generate hand motions, several soft robotic glove designs employed bending soft actuators directly attached to the back of the finger, while others used motors or Pneumatic Artificial Muscles (PAMs) to generate bending motions indirectly via auxiliary mechanisms [10-12]. For the first type, bending motions are generated and applied to the finger in one step, while compliance and safety features are free bi-products thanks to the pneumatic [8, 9] or hydraulic [7] actuation mechanisms. However, without rigid structural elements for conducting force to the fingertip, the force generated at the tip of finger is usually limited to several Newtons [7-9]. In regard to the second type, the cable-driven systems are both light-weight and adaptive in size [11, 12]. Cable-driven systems are widely utilized in surgical robots, robotic hands and arms, where space is a critical concern. However, for wearable robotic devices, the primary incentive in adopting cable-driven mechanism is to take advantage of its natural compliance and adaptability while being able to separate the actuation point and the actuator in order to achieve very low end-effector weight. To achieve this, the routes of cables are fixed at the exterior of hands, and the human hand skeleton is used as structural support. With this mechanism, cable-driven systems are no longer constrained by the geometrical alignment requirement of rigid linkage systems, thus one design/size could cope with multiple users.

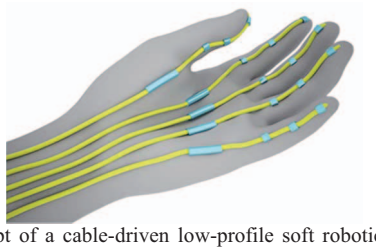

Fig.1. Concept of a cable-driven low-profile soft robotic glove. It is comprised of cables (green) and sheaths (blue). Cables are connected to PAMs mounted on the fore arm that drive the finger off-site.

As for the actuation method, PAMs are chosen over electric motors for their unique set of capabilities and features including spring-like characteristics and their high power to weight ratio [13]. When a PAM is pressurized, its body will contract linearly. Due to air fluidity and compressibility, the pressurized PAM could still be deformed within a limited range around its equilibrium status with an external force applied, which results in flexibility and passive compliance. This unique feature of PAMs makes it advantageous over electric motors for wearable applications, for their superior capability to deal with unexpected human motions. PAMs also have a much higher power to weight ratio than electric motors. For example, the 30mm Air muscle produced by Shadow Company could generate maximum forces up to 700N, while only weighs 80g. This makes PAMs ideal candidates for lightweight high force application scenarios.

In this paper, we are aiming at designing an extra light-weight wearable robotic glove with high adaptability and high dexterity, which will not only release the weight exerted to the users' hand, but also provide high safety to the users, compared to the existing robotic glove. Therefore, a soft robotic glove design based on cable-driven mechanism and PAM actuation is proposed. A conceptual design is illustrated in Fig.1. In this design, each finger is driven

Juan Yi is with the Mechanical Engineering Department, The University of Hong Kong, Hong Kong, China (e-mail: yijuan@connect.hku.hk)

Zhong Shen is with the Mechanical Engineering Department, The University of Hong Kong, Hong Kong, China (e-mail: u3516723@connect.hku.hk)

Chaoyang Song is with the Mechanical and Aerospace Engineering Department, Monash University, Clayton, Australia (e-mail: Chaoyang.Song@monash.edu)

Zheng Wang is with the Mechanical Engineering Department, The University of Hong Kong, Hong Kong, China (phone: 852-59240801; e-mail: zheng.wang@ieee.org)

978-1-4673-8959-4/16/$31.00 © 2016 IEEE

independently with both flexion and extension motions. The cables are tightly fitted to the corresponding fingers with minimal protrusions and no rigid exoskeletal components, hence make the device ultra-low-profile and convenient to use. The PAM technology to drive the glove piece will be presented in Section II, including the fabrication process and the mechanical properties, while the details of the glove piece design will be shown in Section III, backed by an FEM analysis and experimental data about trajectory and force of fingertip in Section IV, where the performance of the glove will also be evaluated by grasping a group of objects of various sizes.

II. Pneumatic Artificial Muscle

Fluidic actuators have been used for many years due to their simple mechanical structures, low-cost actuation source and intrinsic compliance compared to electrical motors. The pneumatic cylinder, the most common-used fluidic actuator, consists of a cylinder acting as an air container and a piston responsible for transmitting axial force. Its force generated from pneumatic cylinder is proportional to the cross section area of the piston, which offers the opportunities to realize simple control. However, constant force also means that higher force output is destined to have higher volume and weight, which will limit its application. The other limiting factor is its high rigidity and density of the metallic components.

Fluidic soft actuators, as one new class of fluidic actuators, usually use light-weight and flexible materials. Both high adaptability and high power to weight ratio over pneumatic cylinders and electric motors are exhibited in soft actuators. Such characteristics make them be used to accomplish a series of dexterous motions, such as grasping fragile objects and crawling locomotion [1-6], which are difficult for traditional robotic devices.

PAM generates motion from compressed air in a completely different approach from air cylinders. A typical PAM consists of an internal soft chamber, an external fiber mesh layer, and pneumatic fittings connecting the inner chamber to the air source [13]. Once the soft chamber is pressurized, the external mesh prevents its over-inflation and transfer radial dilation into axial contraction whilst generating an axial pulling force. By constraining the soft chamber with the mesh, it is possible to withstand high pressure and generate substantial forces. Similar designs were adopted by a list of commercial products [15-17], since it was first applied as actuator in 1960s [14].

A. Materials

The PAM used in this device is comprised of a balloon acting as the internal soft chamber, an external layer of mesh braided with Nylon material, a segment of PU tube used as a pneumatic fitting and Kevlar strands for sealing two ends of body. In addition, stainless cables fastened on both ends provide a convenient way to install the PAM on the device, and also transmit the pulling force to other structures. These components and an assembled PAM are presented respectively in Fig. 2 (a) and Fig. 2 (b). For the materials of the soft chamber and the mesh, an important requirement they need to meet is high anti-fatigue strength, since they both need to sustain high stress. With respect to the pneumatic fitting, the main consideration on choosing it is gas tightness, as the fittings must seal two ends under the situation where PAMs are inflated and loaded. Dimensions of PAMs are decided by the application requirements, such as functions needed to perform and space occupation, based on the mechanical properties which will be investigated below.

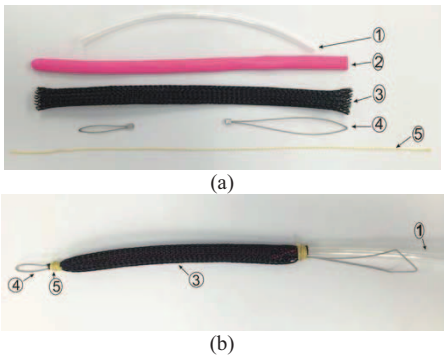

(a)

(b)

Fig.2. (a) Materials of a PAM. 1: a segment of PU tube for connecting to air source. 2: a balloon as the soft chamber. 3: the mesh at the outside of chamber. 4: stainless cables. 5: the Kevlar strands used to avoid air loss. (b) An assembled PAM.

TABLE I. Static Models

Factors	Models
Basic Model [13]	$F = P'b^2(3cos\theta^2 - 1)/(4\pi n^2)$
Thickness of the mesh and the soft chamber [13]	$F = P'b^2(3cos\theta^2 - 1)\Big/\left(4\pi n^2\right) + \pi P'\left[bt_k\left(2\sin\theta - 1/\sin\theta\right)/\pi n - t_k^2\right]$
Irregular cylinderical end-parts [18]	$F_{(\varepsilon,P)} = \pi r_0^2 P\left[a\left(1-k\varepsilon\right)^2 - b\right]$
Dry friction [19]	$F_{friction} = f_s P S_{contact}/S_{scale}$

B. Mechanical Properties

Most previous studies on working principles of PAMs were based on the theory of energy conservation. Chamber thickness, dry friction and effects of end caps were taken into consideration. Here we consider all the factors, and then, build a new static model. Assume the PAM is actuated following an adiabatic process,

$$dW_{out} = dW_{in}, \tag{1}$$

where W_{out} is the system output work and W_{in} is the input work to the system.

Supposing that the PAM keeps in a cylindrical shape with zero-wall thickness, a basic model based on (1) has been developed [13]. However, in practice, the thickness of mesh and the soft chamber affects the axial force according to the previous studies [13]. And the shape of two ends is not a cylinder but a camber with variable sections, which results in a smaller contraction. Additionally, it has also been observed in previous study [13, 19] that the dominated dry friction could not be ignored during contraction. To develop a more precise static model, the factors discussed above have been taken into consideration, which are listed in Table I. Therefore, the axial force F_0 during contracting is described by incorporating the above factors,

$$F_0 = F_1 - F_2, \tag{2}$$

where F_2 is the dry friction [19], F_1 is the static force after considering the thickness and end-parts effects, which is equivalent to

$$F_1 = \frac{Pb^2\left(3a^2-1\right)}{4\pi n^2} + \pi P\left[\frac{bt}{\pi n}\left(2g - \frac{1}{g}\right) - t^2\right], \tag{3}$$

where P is the relative inner pressure of the soft chamber, b is the length of one fiber, C is defined as contraction which is the ratio of displacements in axis direction to the initial length, n is the number of fibers to braid the PAM, t is the thickness of the soft chamber and the mesh, $a = (1 - C/k)\cos\theta_0$, $\sin\{\cos^{-1}\left[(1-C/k)\cos\theta_0\right]\}$, θ_0 is the initial angle between fiber and chamber's long axis, θ is the braided angle with respect to axial direction, and k is the correction factor for decreasing the effects of curved two ends on contraction.

One approach is given to calculate the value of k. Considering our PAM consists of a cylindrical body and two curved end-parts, the contraction of PAM combines the contraction of cylindrical body with the value of end-parts. In this way, k can be expressed as

$$k = O_1/(O_1 + 2O_2) + 2O_2/(O_1 + 2O_2)\lambda \tag{4}$$

where O_1 is the length of the cylindrical body in the initial state, O_2 is the length of one curved end-part in the initial state. λ is considered as a correction factor for the curved end-parts,

$$\lambda = \left[C'_{max}\left(O_1 + 2O_2\right) - C_{max}O_1\right]/\left(2C_{max}O_2\right) \tag{5}$$

where C'_{max} is assumed as the maximum contraction theoretically and C_{max} is considered as the maximum contraction in real circumstance which could be estimated experimentally.

To investigate the maximum contraction from experiments, five samples were tested in free space [13]. These PAMs have the same initial length of 153mm and initial diameter 9.53mm. A load cell (100N max.) was connected to one end of PAM to record the axial force which was controlled to maintain in zero in this experiment. Pressure was supplied to PAM and regulated by an electro-pneumatic regulator (SMC, ITV103, 0.5MPa max.). In the meanwhile, axial displacement was measured through displacement of ball screw driven by a stepper motor (NEMA 57 Stepper Motor, 200 steps per revolution) under different pressure values. The relationship between contraction and pressure can be obtained in Fig.3 (a). If 150kPa pressure was selected to analyze the repeatability of fabrication, we can conclude that our PAM have significantly good repeatability on fabrication with a standard deviation $\sigma = 0.00449$ (1.4% of a maximum contraction of 0.31). Contraction arrives to 31% under 300kPa pressure. Keeping increasing the inner pressure, the maximum contraction was recorded as 33%. Theoretically, the maximum contraction could arrive to 37% [13]. Based on (6) and (7), a k parameter could be calculated equal to 1.12.

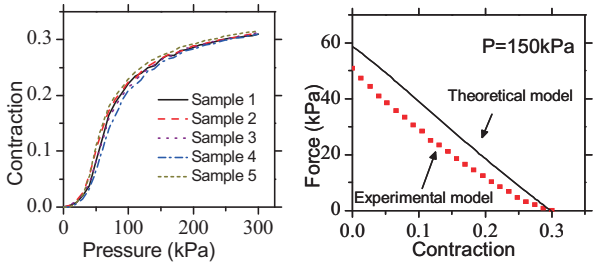

Fig.3. Quasi-static tests. (a) Free space test. Mechanical characteristic in free space is plotted and the repeatability of PAM is investigated with five samples. Contraction is defined as the ratio of the reduced length of artificial muscle to the natural length. (b) Isotonic test. The relationship between axial force and contraction of theoretical and experimental models is presented. ($b = 171mm, \theta_0 = 26.525^\circ, n = 2.55, t = 0.7mm$).

For a given pressure, the experimental results on relationship between static axial force and contraction in Fig. 3 (b) indicate that, in a constant pressure 150kpa, the artificial muscle could generate maximum force reaching to 50N, which should be enough to meet the requirement of 6-10N in fingertip for ADLs, according to previous studies on the cable-driven mechanism [12]. The experimental results also are compared with the calculated results (Fig. 3 (b)). Results show that the PAM generates the maximum force at its initial length. And then, force decreases to zero when it gets to the maximum contraction. This trend is followed by both the experimental and theoretical results. The slight differences between them can be mainly attributed to the non-elasticity of the soft chamber. However, in the theoretical model, an assumption of no extensibility on the soft chamber was made. Therefore, further analysis on the non-linear elastic materials will be built in the future.

III. Design Requirements and Details of Glove

For practical applications, several important factors may affect the performance are needed to be carefully considered, including the weight of device, force capability and high likelihood of grasping action between healthy hand and device. Weight is a very practical consideration for wearable device. Cumbersome devices will significantly affect users' performance and even bring extra loading to the hand. Considering a wearable robotic glove, the weight of the part worn on the hand, involving the cable-driven mechanism, actuators and the glove, should not exceed 0.45Kg [3, 21] to ensure the device could be used by both children and adults. Another key factor for exoskeletal devices is force capability. In this regard linkage-based rigid devices have always held a clear lead against soft opponents. However, it is not the absolute forces that the patents really need: biomechanical studies ranging more than two decades have shown that the majority of simple daily tasks need less than 10N fingertip force [22, 23]. This can be further justified by a simple calculation: in order to grasp and hold an object weighing 1kg (most daily objects would fall into this category), considering the friction coefficient between fingers and daily objects ranges from 0.2 to 0.3 [24], the resulting normal force is 30-50N, which distributes into 6-10N per finger. Therefore, in this work the targeted fingertip force capability is 10N. Also,

TABLE II. PERIMETERS OF INDEX RINGS

Finger sizes	Perimeters of index rings (mm)		
	Index Ring 1	*Index Ring 2*	*Index Ring 3*
Large	62.7	74.1	81.5
Medium	56.5	65.9	71.5
Small	53.3	62.5	68.4
Average	**57.5**	**67.5**	**73.8**

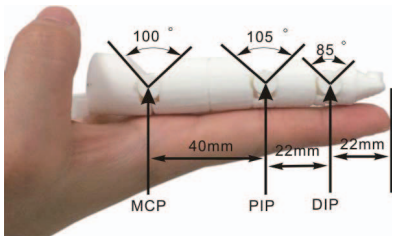

Fig.4. Illustration of index finger. Joints names and ROMs are indicated. The upper model printed with 3D technology will be used in the following tests.

motions matching should be considered as any deviation or conflict between the device and user's hand could significantly affect the performance and even may injure the hand. These key factors will be investigated in the following sections.

Because of the coupling interaction between human hand and the device, an understanding of human fingers structures is important. A healthy hand possesses over 20 degrees of freedom (DOF), of which at least 15 are involved in completing daily tasks. To simplify the analysis, four of the five fingers were considered, except the thumb due to its unique motions. The joints shown in Fig.4 are respectively DIP (distal interphalangeal), PID (Proximal interphalangeal) and MCP (metacarpophalangeal) with at least one DOF each joint, except the MCP exhibits two DOFs. On the basis of the measurements on the joints range of motions (ROMs) [21], finger ROMs of different persons are approximately the same, which could be observed in Fig. 4. Additionally, the lengths of phalanges are varied resulted from the differences on persons' skeletons.

For the design and manufacture of the glove piece, the actuation of each finger took advantage of the inherent adaptability of the cable-drive mechanism and used two antagonistic cables to generate the flexion and extension motions. This is in fact regarding the user's hand skeleton as the structural support and hence eliminating the necessity of any external rigid elements in generating bending motions. However, in order to prevent the cables from detaching, ring fixtures were attached to the finger, one ring per each link. To induce minimum influence to the overall system rigidity, the rings were fabricated using flexible PLA materials. The dimensions of the rings, on the other hand, were customizable. For the reported results the dimensions were taken from experimentally measured finger perimeters of three subjects wearing one glove, as presented in Table II, one male with large hand size, and two females with medium to small hand sizes.

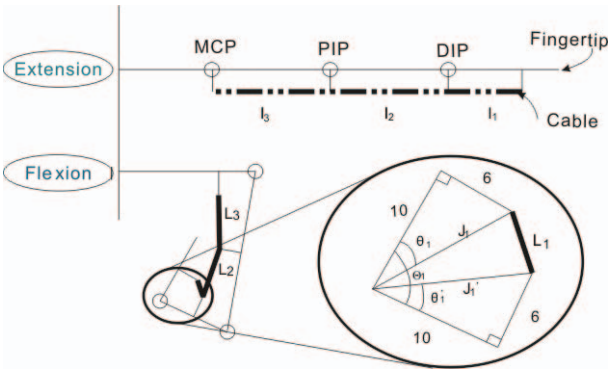

Fig.5. Schematic of the cable travel distance. Extension and flexion states are sketched respectively with dashed lines and solid lines. Travel distance is calculated by subtracting the flexion length of cable (dashed) from the original length (solid).

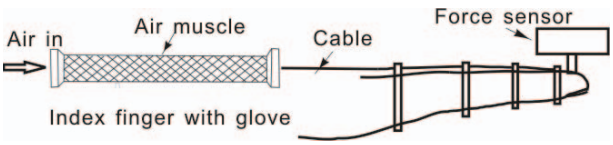

Fig.6. Schematic of experimental settings. The glove was mounted on the platform with the palm up. The relationship between fingertip force and pressure was recorded.

As actuators for the glove, PAMs were fastened on the fore arms via hook and loops for distributing the weight applied to the hand and ensuring the compliance of the device with users. In regard to the lengths of PAMs, they actually were decided by the travel distances of cables, the length of fore arm and other factors. The travel distance under flexion was calculated geometrically (Fig. 5),

$$D = \sum_{i=1}^{3} (l_i - L_i) \tag{6}$$

where $\sum_{i=1}^{3} l_i$ is the length of cable's one part in extension, $\sum_{i=1}^{3} L_i$ is the length of cable in flexion, D is the travel distance of the cable for index finger. L_1 can be represented as

$$L_1 = \sqrt{J_1^2 + J_1'^2 - 2J_1J_1' \cos\left(\Theta_1 - \theta_1 - \theta_1'\right)} \ . \tag{7}$$

Another practical consideration on deciding the length of PAM is the length of users' fore arms, which should satisfy

$$L_0 \le \beta L_A \ , \tag{8}$$

where L_0 is the length of PAM, L_A is fore arm's length and β is a safety factor used to reserve the space for the wrist and arm-joint motion to avoid any conflict between the device and the arm. Furthermore, based on the properties of PAM, L_0 could be calculated as

$$L_0 C'_{max} = \alpha D \tag{9}$$

where the C'_{max} is the maximum contraction of PAM measured by experiments. α is the efficiency of cable-driven mechanism. Therefore, from (6), L_0 can be represented as

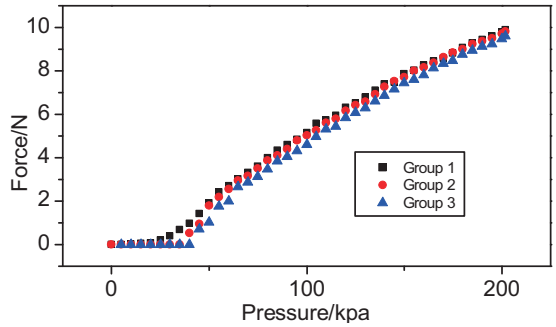

Fig.7. Relationship between fingertip force and pressure. Three groups with same experimental settings results are plotted.

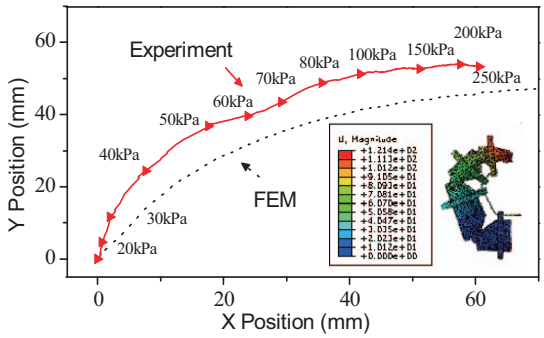

Fig.8. Trajectory of fingertip in free space. The X-Y position of FEM model and experimental model are compared.

$$L_0 = \alpha \sum_{i=1}^{3} (l_i - L_i) / C'_{max} \tag{10}$$

where $L_0 \le \beta L_A$ should be satisfied.

IV. Experiments and Performance Evaluation

A. Experiments on Fingertip Force

In order to estimate the fingertip force experimentally, a test platform was developed (Fig. 6) with an integrated air pressure regulator and a load cell. Also, to simulate the interference between glove and wearers by experiments, a finger model (Fig.4) made by 3D printing using strong PLA materials was used in our experiments. Its lengths and ROMs were the same with the index finger in Fig. 4. The index finger model wearing the glove was mounted on the test platform horizontally. When the PAM were inflated with compressed air, the proximal distal of finger model would be constrained, thus generating a vertical force. The input pressure of PAM was increased to 200kPa with an increment of 5kpa and the magnitude of force generated in the fingertip was recorded (Fig. 7). The fingertip force was measured approximating to 10N under 200kPa pressure, which is enough to perform daily tasks. It is also noted that the force is globally proportional to the pressure. The relationship between force and pressure shows similarity with PAM. Therefore, higher force could be easily achieved by increasing the input pressure.

B. Experiments on Fingertip Trajectory

To explore motions of healthy hand and device, trajectory of fingertip was studied. A test setup on investigating the trajectory of fingertip in free space was developed. The finger model wearing the glove was fastened on a platform horizontally with the finger model bending upwards without

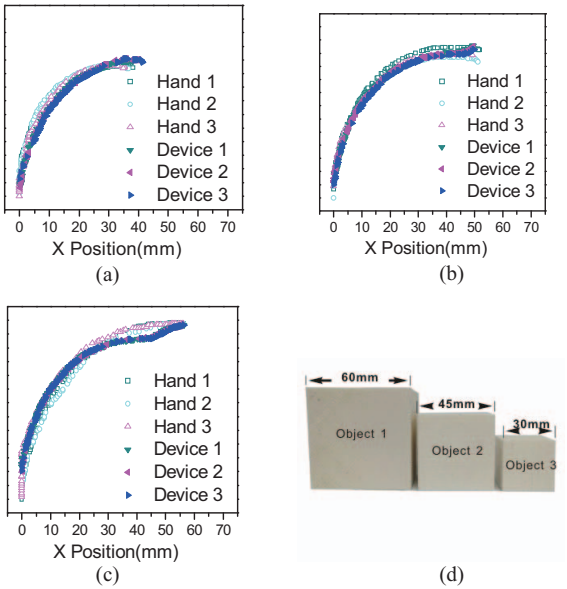

Fig.9. (a)-(c) Comparison of fingertip trajectory between finger model wearing the device and human finger when grasping a series of cubes. Three times results for each grasping test are plotted. The dimensions of finger model are the same with the subject. (a) Grasp object 1. (b) Grasp object 2. (c) Grasp object 3. (d) Objects.

obstacles. Trajectories of fingertip were recorded under increased pressure. The finite element simulation on exploring the trajectory was modeled using the Abaqus 6.13 (SIMULIA) with Explicit Model. Both the average experimental data of three groups at gradually increasing pressure and the simulation results by the FEM are shown in Fig. 8. Results show that the measured trajectory and simulation results are well-matched. Therefore, same experimental settings could be applied to the following tests.

Based on the conclusions above, a series of grasping tests were conducted to further make comparison between the motions of the device and the healthy human finger on trajectories. Three cubes (Fig. 9 (d)) with different sizes were employed in the experiments. To avoid any forceful contact between subjects and objects, objects were fixed on a platform horizontally which was positioned above the table, where both the hand and the model were arranged with palms facing up. The position of hand and distance from the table to platform are preset values which have been tested and modified in advance. In the experiments, a camera was used to capture the trajectory of fingertip. The comparison between experimental results from different groups are plotted in Fig. 9 which demonstrates that the performance of glove when grasping different things is well in accordance with real circumstance. The ratio of curved area under finger model's trajectory to the area under trajectory of human natural motion was calculated to evaluate the matching degree. By comparing Fig. 9 (a), (b) and (c) respectively: 98.0%, 87.2%, and 79.6%, Therefore, we can conclude that a better performance was achieved on grasping relatively big size object.

C. Glove Evaluation

The device in this paper consists of the glove piece, actuators located on the fore arm and other electro-mechanical components (pneumatic components, power supplies and

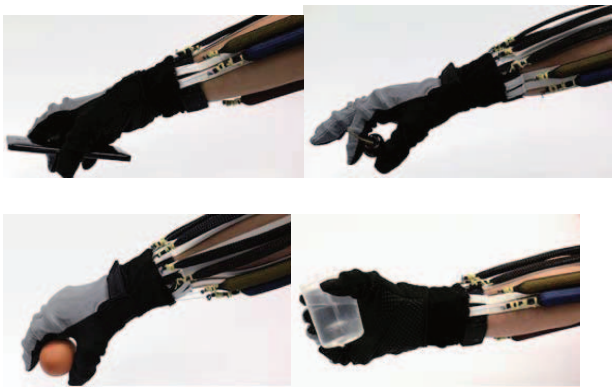

Fig.10. Demonstration on pinching and grasping various objects: a cherry, an egg, a mobile phone and a cup of water.

controllers). The total weight of the glove and actuators is 0.161kg, of which the part applied to the hand does not exceed 0.1kg. Comparing with the majority of previous devices [1-5, 7, 8, 20] applying 0.15Kg-0.25Kg weight to the hand, our glove shows superiority on lightness. This weight is almost the same with a leather glove.

For further evaluating the ability of providing assistance performance towards ADLs, several objects that have varied shapes and stiffness were prepared to be grasped or pinched by a user wearing the glove. A supply of compressed air was inflated to the PAMs with an increment of 10kPa, which resulted in a flexion motion. After the designated tasks being completed, the rest PAMs were triggered to pull the fingers back. The good performance has been demonstrated in Fig. 10 (b).

V. Conclusion and Future Works

A wearable robotic glove based on cable-driven mechanism and PAM actuation is proposed in this paper. PAMs were fabricated, and analyzed by using experimental and analytical methods which demonstrate the unique mechanical properties of PAMs. To evaluate the capability of the device to assist users in ADLs, both the fingertip force and the trajectory of finger motion were studied experimentally. High enough force was proved to be provided. And well-matched motion with human hand was presented. In addition, the FEM simulation on finger motion was developed to validate the experimental results. Finally, demonstrations on grasping and pinching the objects that users may encounter were presented with one person wearing the glove.

In the future, much more degrees of freedom for each finger will be involved to improve the flexibility of fingers, since the glove has only one degree for MCP joints currently. Furthermore, in the next version of glove, designs on mimicking the complicated motions of thumb will be involved to enhance the capability of the glove.

References

[1] M. Fontana, A. Dettori, F. Salsedo, and M. Bergamasco, "Mechanical design of a novel Hand Exoskeleton for accurateforce displaying," *Proc. of the 2009 IEEE Int. Conf. on Robotics and Automation,* pp. 1704-1709.

[2] S. Nakagawara, H. Kajimoto, N. Kawakami, S. Tachi, and I. Kawabuchi, "An Encounter-Type Multi-Fingered Master Hand Using Circuitous Joints," *Proc. of the 2005 IEEE Int. Conf. on Robotics and Automation,* pp. 2667-2672.

[3] P. M. Aubin, H. Sallum, C. Walsh, L. Stirling and A. Correia, "A pediatric robotic thumb exoskeleton for at-home rehabilitation: the Isolated Orthosis for Thumb Actuation (IOTA)," Int. J. Intelligent Computing and Cybernetics, vol. 7, no. 3, pp. 233-252, 2014.

[4] M. Fontana, A. Dettori, F. Salsedo and M. Bergamasco, "Mechanical design of a novel Hand Exoskeleton for accurate force displaying," in *2009 IEEE Int. Conf. Robotics and Automation,* pp. 1704-1709.

[5] F. Ilievski, A. D. Mazzeo, R. F. Shepherd, X. Chen and G. M. Whitesides, "Soft robotics for chemists," *J. Angewandte Chemie,* vol. 123, no. 8, pp. 1930-1935, 2011.

[6] Z. Wang, Z. Q. Chen and J. Yi, "Soft robotics for engineers," HKIE Transactions, vol. 22, no. 2, pp. 88-97, 2015.

[7] P. Polygerinos, S. Lyne , Z. Wang, L. Fernando, Nicolini, B. Mosadegh, G. M. Whitesides and C. J. Walsh, "Towards a Soft Pneumatic Glove for Hand Rehabilitation," in *2013 IEEE Int. Conf. Intelligent Robots and Systems,* pp. 2153-0858.

[8] P. Polygerinos, Z. Wang, K. C. Galloway, R. J.Wood, C. J. Walsh, "Soft robotic glove for combined assistance and at-home rehabilitation," *J. Robotics and Autonomous Systems,* in press.

[9] T. Noritsugu, H. Yamamoto, D. Sasaki and M. Takaiwa, "Wearable Power Assist Device for Hand Grasping Using Pneumatic Artificial Rubber Muscle," *J. Robot and Human Interactive Communication,* pp. 655-660, 2004.

[10] E. J. Koeneman, R. S. Schultz, S. L. Wolf, D. E. Herring and J. B. Koeneman, "A Pneumatic Muscle Hand Therapy Device," in *26th Annu. Int. Conf. 2004 IEEE. Eng. Medicine and Biology Society,* pp. 2711-2713.

[11] Y. Mao and S. K. Agrawal, "A Cable Driven Upper Arm Exoskeleton for Upper Extremity Rehabilitation," in *2011 IEEE Int. Conf. Robotics and Automation,* pp. 4163-4168.

[12] H. K. In, K. J. Cho, K. R. Kim and B. S. Lee, "Jointless Structure and Under-Actuation Mechanism for Compact Hand Exoskeleton," in *2011 IEEE Int. Conf. Rehabilitation and Robotics,* pp. 1945-7898.

[13] C. P. Chou and B. Hannaford, "Measurement and modeling of McKibben pneumatic artificial muscles," *IEEE Trans. Robotics and Automation,* vol. 12, no. 1, pp. 90-102, 1996.

[14] L. M. Joseph, "Artificial muscle," *Life.* pp 87-88, 1960.

[15] Bridgestone Corporation, Tokyo, Japan, Soft Arm ACFAS Robot System, 1987.

[16] Festo Company, Germany, Fluidic Muscle, http://www.festo.com.

[17] Shadow Robot Group, London, UK, The shadow Air Muscle, http://www.shadow.org.uk.

[18] B. Tondu and P. Lopez, "Modeling and control of McKibben artificial muscle robot actuators," *IEEE J. Control Systems,* vol. 20, no. 2, pp. 15-38, 2000.

[19] S. Davis and D. G. Caldwell, "Braid Effects on Contractile Range and Friction Modeling in Pneumatic Muscle Actuators," *Int. J. Robotics Research,* vol. 25, no. 4, pp. 359-369, April 2006.

[20] E. Kreighbaum and K. Barthels, *Biomechanics: A Qualitative Approach for studying Human Movement,* Nov 1995.

[21] M. C. Hume, H. Gellman, H. McKellop and R. H. Brumfield, "Functional range of motion of the joints of the hand," *J. Hand Surgery,* vol. 15, no. 2, pp. 240-243, March 1990.

[22] N. Smaby, M. E. Johanson, B. Baker, D. E. Kenney, W. M. Murray and V. R. Hentz, "Identification of key pinch forces required to complete functional tasks," *J. Rehabilitation Research and Development,* vol. 41, no. 2, pp. 215-224, 2004.

[23] K. N. An, E. Y. Chao, W. P. Cooney, and R. L. Linscheid, "Forces in the Normal and Abnormal Hand," *J. Orthopaedic Research,* vol. 3, no. 2, pp. 202–211, 1985.

[24] K. Matheus and A. M.Dollar, "Benchingmarking Grasping Manipulation: Properties of Objects of Daily Living," in *2010 IEEE Int. Conf. Intelligent Robots and Systems,* pp. 5020-5027.